Unbalanced fourth-order interference beyond coherence time

Z. Y. Ou [1,*] and Xiaoying Li [2,†]

[1]*Department of Physics, City University of Hong Kong, 83 Tat Chee Avenue, Kowloon, Hong Kong*

[2]*College of Precision Instrument and Opto-Electronics Engineering, Key Laboratory of Opto-Electronics Information Technology, Ministry of Education, Tianjin University, Tianjin 300072, People's Republic of China*

Interferometry has been used widely in sensing application. However, the technique is limited by the finite coherence time of the light sources when the interference paths are not balanced. Higher-order interference effects involve intensity correlations between multiple detectors and may have the advantage over the traditional second-order interference effect exhibited in only one detector. We discuss various scenarios with unbalanced delays in different paths in fourth-order interference exhibited in coincidence between two detectors. We find, in some cases, interference effect persists even when the delays are much larger than the coherence time of the sources. We also extend the discussion to nonstationary pulsed fields, which need to consider the pulse shape and require a different treatment. These results will be useful in remote sensing applications.

I. INTRODUCTION

Interferometry is the major technique for optical sensing applications [1]. It depends on the optical coherence of light to produce phase-sensitive interference effect in order to achieve high sensitivity and precision [2]. This requires the balance of interferometer paths to within the coherence length of the optical field. But this may limit the scope of applications in remote sensing when a large imbalance of paths exists.

A traditional interference effect depends on second-order coherence of the amplitudes of the fields and involves intensity measurement by only one detector, whereas fourth-order interference involves quantities in the fourth order of field amplitudes and is exhibited in the correlation between intensities measured by two detectors. It was well known that fourth-order interference such as the Hong-Ou-Mandel (HOM) interference effect [3,4] does not rely on the coherence time of the fields in that interference even between independent fields may occur [5,6]. But such effect is insensitive to phase change of the fields. On the other hand, a phase-dependent fourth-order interference effect occurs in Franson interferometer [7], which consists of two highly imbalanced interferometers beyond coherence length [8–10]. But it was shown that the effect exists only for two-photon quantum fields and disappears for stationary classical fields in time-unresolved coincidence measurement [11]. The progress on the interference with imbalanced paths was halted until

recently when it was reported that phase dependent fourth-order interference between two thermal fields can appear in the time-resolved coincidence between two detectors even when the path imbalance of the interferometer is well beyond the coherence length of the fields [12,13]. This leads to a huge advantage over the traditional interferometers based on second-order interference where interference appears in one detector and requires the path imbalance between interfering fields to be smaller than the coherence length of the fields.

Furthermore, even though HOM interference effect is independent of phase difference, it relies on mode match between the two input fields for photon indistinguishability required by quantum interference. Thus the size of the effect is sensitive to the distortion of the wave forms of the input fields. This is especially the case when the fields are in the form of ultrashort pulses and can be a tool for sensing the change of the optical paths in the medium of propagation [6,14].

In this paper, we discuss various scenarios in fourth-order interference with different correlation between interfering fields and unbalanced delays in different paths. We find, in some cases, interference effect persists even when the delays are much larger than the coherence time of the sources. We also extend the discussion to nonstationary pulsed fields, which require the overlap of interfering pulses. The paper is organized as follows. We start by considering in Sec. II the general schemes with stationary fields. In Sec. III, we concentrate on some special scenarios with different correlation between interfering fields and different delays for unbalanced interferometers. We consider the pulsed nonstationary fields in Sec. IV and conclude with a discussion in Sec. V.

*jeffou@cityu.edu.hk

†xiaoyingli@tju.edu.cn

II. GENERAL CASE OF STATIONARY FIELDS

Let us consider the general case of fourth-order interference between two stationary fields $V_{10}(\mathbf{r}, t)$, $V_{20}(\mathbf{r}, t)$. The quantities involved are related to the product of four field
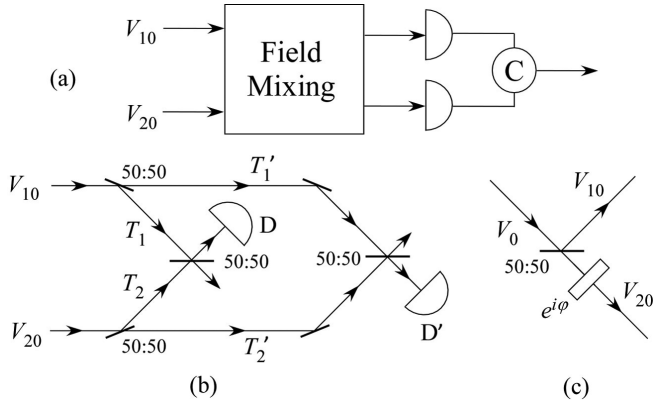
FIG. 1. (a) General scheme of fourth-order interference between two fields by field mixing. (b) A specific scheme of field mixing by using beam splitters. (c) Generation of two fields with a random phase φ from one field by a beam splitter.

amplitudes such as $\langle V_{10}^*(\mathbf{r}_1, t_1) V_{20}^*(\mathbf{r}_2, t_2) V_{10}(\mathbf{r}_1', t_1') V_{20}(\mathbf{r}_2', t_2') \rangle$. This requires intensity correlation measurement by coincidence between two different detectors. To achieve this, we first mix the fields with some linear optics and send the mixed fields to two detectors for intensity correlation measurement (C), as shown in Fig. 1(a). The simplest way of field mixing is by beam splitters. A typical scheme is shown in Fig. 1(b), which will be the scheme of our discussion in this paper. In order to concentrate on fourth-order effect and avoid the confusion with lower order interference, that is, the interference at each detector's output, we assume that there is no phase coherence between $V_{10}(\mathbf{r}, t)$, $V_{20}(\mathbf{r}, t)$, so that $\langle V_{10}(\mathbf{r}, t) V_{20}(\mathbf{r}, t) \rangle = 0$, $\langle V_{10}^*(\mathbf{r}, t) V_{20}(\mathbf{r}, t) \rangle = 0$. In the case of fields of independent origins, this is automatically satisfied. On the other hand, the two fields may originate from one field $V_0(\mathbf{r}, t)$ via splitting by a beam splitter: $V_{10}(\mathbf{r}, t) \propto V_0(\mathbf{r}, t)$, $V_{20}(\mathbf{r}, t) \propto V_0(\mathbf{r}, t) e^{i\varphi}$, as shown in Fig. 1(c). In this case, we introduce a random phase φ in field V_{20} that averages out the second-order interference between V_{10} and V_{20}.

For simplicity without loss of generality, we assume the fields are one dimensional so we can absorb the position variable z with time and only consider the temporal variable t. Then, the general format of the fourth-order quantities are in the form of $\langle V_{10}^*(t_1) V_{20}^*(t_2) V_{10}(t_1') V_{20}(t_2') \rangle$. In particular, cross terms like $\langle V_{10}^*(t_1) V_{20}^*(t_2) V_{10}(t_2) V_{20}(t_1) \rangle$ and $\langle V_{10}^*(t_1) V_{20}^*(t_1) V_{10}(t_2) V_{20}(t_2) \rangle$ result in fourth-order interference.

In order to obtain the interference terms mentioned above, we introduce various delays T_1, T_2, T_1', T_2' to account for different times of t_1, t_2, t_1', t_2'. Different values of T_1, T_2, T_1', T_2' lead to different scenarios of interference. For example, when $T_1 = T_1', T_2 = T_2'$, this scheme is simply a Hong-Ou-Mandel interferometer for two fields V_{10}, V_{20}. When V_{10}, V_{20} originate from V_0 as shown in Fig. 1(c), this scheme was shown [4] to be able to measure the coherence time of V_0.

For the general scheme in Fig. 1(b), the fields at two detectors can be expressed as

$$V(t) = [V_{10}(t + T_1) + V_{20}(t + T_2)]/2,$$
$$V'(t) = [V_{10}(t + T_1') - V_{20}(t + T_2')]/2. \quad (1)$$

The coincidence measurement is related to $\langle I(t) I'(t + \tau) \rangle$ with

$$I \equiv |V(t)|^2 \propto |V_{10}|^2 + |V_{20}|^2 + V_{10}^* V_{20} + V_{20}^* V_{10},$$
$$I' \equiv |V'(t + \tau)|^2 \propto |V_{10}'|^2 + |V_{20}'|^2 - V_{10}^{*'} V_{20}' - V_{20}^{*'} V_{10}',$$
$$(2)$$

where $V_{10} \equiv V_{10}(t + T_1)$, $V_{20} \equiv V_{20}(t + T_2)$, $V_{10}' \equiv V_{10}(t + T_1' + \tau)$, and $V_{20}' \equiv V_{20}(t + T_2' + \tau)$. Expanding $\langle I(t) I'(t + \tau) \rangle$ and keeping in mind the random phase $e^{i\varphi}$, we have

$$\langle I(t) I'(t + \tau) \rangle \propto \langle (|V_{10}|^2 + |V_{20}|^2)(|V_{10}'|^2 + |V_{20}'|^2) \rangle$$
$$- \langle (V_{10}^* V_{20} + V_{20}^* V_{10})(V_{10}^{*'} V_{20}' + V_{20}^{*'} V_{10}') \rangle, \quad (3)$$

where, because of the random phase $e^{i\varphi}$, the unpaired cross terms like $\langle |V_{10}|^2 V_{20}^* V_{10} \rangle$, etc., are zero. Expanding Eq. (3), we have

$$\langle I(t) I'(t + \tau) \rangle \propto \langle I_{10} I_{10}' \rangle + \langle I_{20} I_{20}' \rangle + \langle I_{10} I_{20}' \rangle + \langle I_{20} I_{10}' \rangle$$
$$- (\langle V_{10}^* V_{20} V_{20}^{*'} V_{10}' \rangle + \text{c.c.}) - (\langle V_{10}^* V_{20} V_{10}^{*'} V_{20}' \rangle + \text{c.c.}), \quad (4)$$

where c.c. means complex conjugate. Obviously, $\langle V_{10}^* V_{20} V_{20}^{*'} V_{10}' \rangle$ and $\langle V_{10}^* V_{20} V_{10}^{*'} V_{20}' \rangle$ are the interference terms. Again, because of the random phase $e^{i\varphi}$, term $\langle V_{10}^* V_{20} V_{10}^{*'} V_{20}' \rangle$ and its complex conjugate are normally zero. The nonzero term can be explicitly written as

$$\langle V_{10}^* V_{20} V_{20}^{*'} V_{10}' \rangle = \langle V_{10}^*(t + T_1) V_{20}(t + T_2)$$
$$\times V_{20}^*(t + T_2' + \tau) V_{10}(t + T_1' + \tau) \rangle. \quad (5)$$

The evaluation of the nonvanishing interference term in Eq. (5) requires the knowledge of the statistics of field fluctuations. For example, Gaussian statistics of thermal fields will break the four-term average into a two-term average: $\langle V_{10}^* V_{20} V_{20}^{*'} V_{10}' \rangle_{th} = \langle V_{10}^* V_{20} \rangle \langle V_{20}^{*'} V_{10}' \rangle + \langle V_{10}^* V_{10}' \rangle \langle V_{20} V_{20}^{*'} \rangle + \langle V_{10}^* V_{20}^{*'} \rangle \langle V_{20} V_{10}' \rangle$. But we cannot go further for general fields without some approximations. Next, we will consider those approximations that lead to different scenarios in fourth-order interference.

III. VARIOUS SCENARIOS

A. Scenarios with different field correlations

The easiest approximation is to assume that there is no correlation between V_{10} and V_{20} fields. Then, Eq. (5) becomes

$$\langle V_{10}^* V_{20} V_{20}^{*'} V_{10}' \rangle = \langle V_{10}^*(t + T_1) V_{10}(t + T_1' + \tau) \rangle$$
$$\times \langle V_{20}(t + T_2) V_{20}^*(t + T_2' + \tau) \rangle$$
$$= I_{10} I_{20} \gamma_{11}(\tau - \Delta T_1) \gamma_{22}^*(\tau - \Delta T_2), \quad (6)$$

with $I_{j0} \equiv \langle |V_{j0}(t)|^2 \rangle$, $\Delta T_j \equiv T_j - T_j'$, and

$$\gamma_{jj}(\tau) \equiv \langle V_{j0}^*(t) V_{j0}(t + \tau) \rangle / I_{j0} \quad (j = 1, 2) \quad (7)$$

as the second-order coherence functions of V_{10}, V_{20}, respectively. With this, Eq. (4) becomes

$$\langle I(t) I'(t + \tau) \rangle \propto I_{10}^2[1 + \lambda_1(\tau)] + I_{20}^2[1 + \lambda_2(\tau)]$$
$$+ 2 I_{10} I_{20}[1 - |\gamma_{11} \gamma_{22}| \cos(\varphi_{11} - \varphi_{22})], \quad (8)$$
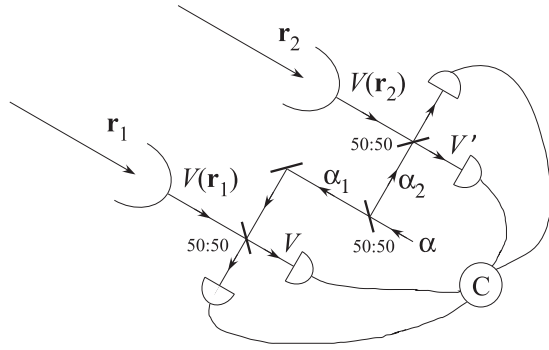
FIG. 2. Schemes of fourth-order interference for application in astronomy.

where $\lambda_j \equiv \langle I_j I_j' \rangle / I_{j0}^2 - 1$ $(j = 1, 2)$ is the normalized autointensity correlation, describing the intensity fluctuations. $|\gamma_{jj}|, \varphi_{jj}$ are the magnitude and phase of γ_{jj}.

This scenario occurs when V_{10} and V_{20} come from independent sources such as two celestial objects in the sky. $\varphi_{11} - \varphi_{22}$ contains information to resolve these two objects as in two-photon amplitude astronomy [15].

Another scenario is when V_{20} is from an ultrastable coherent source or coherent state, that is, $V_{20} = \alpha$. In this case, V_{20} can be thought of as a weak local oscillator and it was first discussed in the context of single-photon nonlocality [16]. An application is in optical stellar interferometry for astronomy [17]. We treat the case in the following.

The goal of stellar interferometry is to measure the normalized second-order coherence function [2] $\gamma(\mathbf{r}_1, \mathbf{r}_2, \tau) \equiv \langle V^*(\mathbf{r}_1, t)V(\mathbf{r}_2, t + \tau) \rangle / \sqrt{\langle |V(\mathbf{r}_1, t)|^2 \rangle \langle |V(\mathbf{r}_2, t)|^2 \rangle}$ of the stellar optical field $V(\mathbf{r}, t)$ at two locations $\mathbf{r}_1, \mathbf{r}_2$. Knowledge of $\gamma(\mathbf{r}_1, \mathbf{r}_2, \tau)$ for a large separation of $\mathbf{r}_1, \mathbf{r}_2$ will lead to high angular resolution by a Fourier transformation [17]. Denote the incoming field at the two locations as $V(t) \equiv V(\mathbf{r}_1, t)$, $\bar{V}(t) \equiv V(\mathbf{r}_2, t)$, which are equivalent to $V_1(t + T_1), V_1(t + T_1')$ with different delays in Fig. 1(b). We mix them with local oscillator fields denoted by α_1, α_2, respectively, which are split from a common stable source of α (equivalent to V_{20} in Fig. 1), as shown in Fig. 2. So the fields at the detectors are

$$V(t) = [V(t) + \alpha_1]/\sqrt{2}, \quad V'(t) = [\bar{V}(t) + \alpha_2]/\sqrt{2}. \quad (9)$$

The delay of wave front between the two detectors is included in positions $\mathbf{r}_1, \mathbf{r}_2$. The intensity correlation measurement gives

$$
\begin{aligned}
\langle I(t)I'(t+\tau) \rangle &= \langle |V(t)|^2 |V'(t+\tau)|^2 \rangle \\
&\propto \langle |V(t)|^2 |\bar{V}(t+\tau)|^2 \rangle + I|\alpha_2|^2 + \bar{I}|\alpha_1|^2 \\
&\quad + |\alpha_1\alpha_2|^2 + \langle V^*(t)\bar{V}(t+\tau) \rangle \alpha_1\alpha_2^* \\
&\quad + \langle V(t)\bar{V}^*(t+\tau) \rangle \alpha_1^*\alpha_2 \\
&= I\bar{I}[1 + \bar{\lambda}(\tau)] + |\alpha_1\alpha_2|^2 + [I|\alpha_2|^2 + \bar{I}|\alpha_1|^2] \\
&\quad \times [1 + \xi|\gamma(\tau)|\cos(\varphi_\gamma + \Delta\phi_\alpha)], \quad (10)
\end{aligned}
$$

where $\xi \equiv 2|\alpha_1\alpha_2|\sqrt{I\bar{I}}/(I|\alpha_2|^2 + \bar{I}|\alpha_1|^2)$, with $I \equiv \langle |V|^2 \rangle$, $\bar{I} \equiv \langle |\bar{V}|^2 \rangle$, $\gamma(\tau) \equiv \gamma(\mathbf{r}_1, \mathbf{r}_2, \tau)$, $e^{i\varphi_\gamma} \equiv \gamma/|\gamma|$, $\Delta\phi_\alpha \equiv \phi_{\alpha_2} - \phi_{\alpha_1}$, and $1 + \bar{\lambda}(\tau) \equiv \langle |V(t)|^2 |\bar{V}(t+\tau)|^2 \rangle / I\bar{I}$.

In deriving Eq. (10), we assume $\alpha_{1,2}$ has stable phases and the incoming fields $V, \bar{V}$ have random phases. Normally, stellar fields have $I = \bar{I}$ and are of thermal nature, so $\bar{\lambda}(\tau) = |\gamma(\tau)|^2$. Setting $|\alpha_1|^2 = |\alpha_2|^2 = I = \bar{I}$ in Eq. (10), we have

$$\langle I(t)I'(t+\tau) \rangle \propto I^2[4 + |\gamma|^2][1 + \mathcal{V}\cos(\varphi_\gamma + \Delta\phi_\alpha)], \quad (11)$$

where $\mathcal{V} \equiv 2|\gamma(\tau)|/[4 + |\gamma(\tau)|^2]$.

With stable local oscillators α_1, α_2, we can measure complex quantity $\gamma(\tau)$ from the two-photon interference fringe to achieve stellar interferometry in astronomy. Note that this scheme is similar to the homodyne measurement technique in stellar interferometry but the photon counting technique is used here to avoid the shot noise problem [18]. However, this method requires time resolution of the detectors better than coherence time in order to measure $\gamma(\tau)$ and thus limits the bandwidth, in a similar way to intensity interferometry [19]. On the other hand, intensity interferometry can be modified by involving fourth-order interference to not require time resolution of the detectors. This is a scenario to be discussed later [Sec. IIIB, scenario (iv)].

B. Scenarios with different delays

All random variables have some correlation time beyond which the fields are not related anymore. So, depending on the relationship between T_1, T_2, T_1', T_2' as compared to coherence time T_c of the fields and resolving time T_R of detectors, we can make some approximations and have different scenarios of fourth-order interference, which give rise to different applications. We categorize them as follows.

(i) $T_1 \sim T_2$ and $T_1' \sim T_2'$, but $|(T_1, T_2) - (T_1', T_2')| \gg T_c, T_R$. This is exactly the scenario depicted in Fig. 1(b). In this case, quantities $V_{10}^*(t + T_1)V_{20}(t + T_2)$ and $V_{20}^*(t + T_2' + \tau)V_{10}(t + T_1' + \tau)$ are well separated in time beyond any correlation time of the fields so that they are independent and we have

$$
\begin{aligned}
&\langle V_{10}^*(t+T_1)V_{20}(t+T_2)V_{20}^*(t+T_2'+\tau)V_{10}(t+T_1'+\tau) \rangle \\
&\approx \langle V_{10}^*(t+T_1)V_{20}(t+T_2) \rangle \\
&\quad \times \langle V_{20}^*(t+T_2'+\tau)V_{10}(t+T_1'+\tau) \rangle \\
&= \Gamma_{12}(\Delta T)\Gamma_{12}^*(\Delta T'), \quad (12)
\end{aligned}
$$

where $\Delta T \equiv T_2 - T_1$, $\Delta T' \equiv T_2' - T_1'$, and $\Gamma_{12}(\Delta T) \equiv \langle V_{10}^*(t + T_1)V_{20}(t + T_2) \rangle$. Notice that this term is normally zero because we assume that there is no coherence between V_{10} and V_{20} or we introduce a random phase between them in the case of common origin so that $\Gamma_{12}(\Delta T) = 0$. But, in the latter case, the random phase is canceled in the product of $\Gamma_{12}(\Delta T)\Gamma_{12}^*(\Delta T')$, as long as the phase changes slowly within the time period of $|T_1 - T_1'|$. So, we will keep this term for the case when V_{10} and V_{20} are from a common origin as shown in Fig. 1(c). Moreover, because $|(T_1, T_2) - (T_1', T_2')| \gg T_c, T_R$, there is no intensity correlation between unprimed quantities and primed quantities, that is, $\langle I_{i0}I_{j0}' \rangle \approx \langle I_{i0} \rangle \langle I_{j0}' \rangle = I_{i0}I_{j0}$. So, with the definition of $\gamma_{12} \equiv \Gamma_{12}/\sqrt{I_{10}I_{20}}$, the overall coincidence measurement result is

$$
\begin{aligned}
\langle I(t)I'(t+\tau) \rangle &\propto I_{10}^2 + I_{20}^2 + 2I_{10}I_{20} \\
&\quad - I_{10}I_{20}[\gamma_{12}(\Delta T)\gamma_{12}^*(\Delta T') + \text{c.c.}] \\
&= I_{10}^2 + I_{20}^2 + 2I_{10}I_{20}\{1 - |\gamma_{12}(\Delta T)\gamma_{12}^*(\Delta T')| \\
&\quad \times \cos[\omega(\Delta T - \Delta T') + \Delta\varphi]\}. \quad (13)
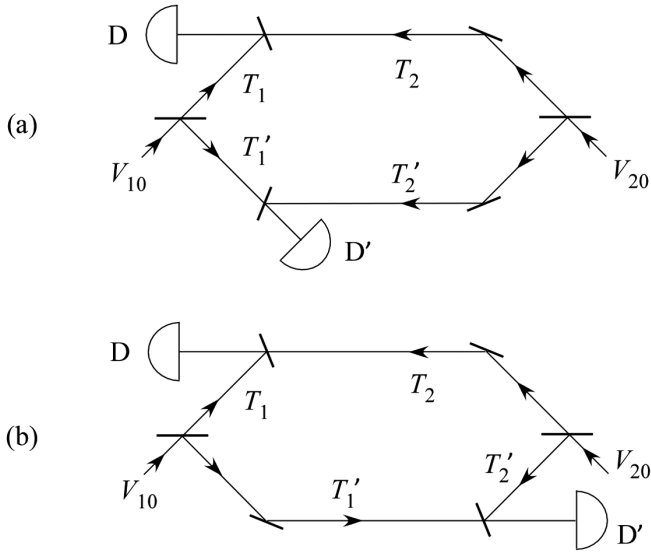\end{aligned}
$$

FIG. 3. Schemes of fourth-order interference between two fields with (a) $T_1 \sim T_1'$ and $T_2 \sim T_2'$, but $|(T_1, T_1') - (T_2, T_2')| \gg T_c, T_R$ [scenario (ii)], and (b) $T_1 \sim T_2'$ and $T_2 \sim T_1'$, but $|(T_1, T_2') - (T_2, T_1')| \gg T_c, T_R$ [scenario (iii)].

This gives rise to fourth-order interference. Notice that the interference fringe does not depend on τ.

(ii) $T_1 \sim T_1'$ and $T_2 \sim T_2'$, but $|(T_1, T_1') - (T_2, T_2')| \gg T_c, T_R$. This scenario is depicted in Fig. 3(a). Similar to scenario (i), we have

$$
\begin{aligned}
\langle V_{10}^*(t &+ T_1)V_{20}(t + T_2)V_{20}^*(t + T_2' + \tau)V_{10}(t + T_1' + \tau)\rangle \\
&\approx \langle V_{10}^*(t + T_1)V_{10}(t + T_1' + \tau)\rangle \\
&\quad \times \langle V_{20}^*(t + T_2' + \tau)V_{20}(t + T_2)\rangle \\
&= \Gamma_{11}(\Delta T_1 + \tau)\Gamma_{22}^*(\Delta T_2 + \tau),
\end{aligned}
\tag{14}
$$

where $\Delta T_1 \equiv T_1' - T_1$, $\Delta T_2 \equiv T_2' - T_2$, and $\Gamma_{jj}(\Delta T_j) \equiv \langle V_{j0}^*(t + T_j)V_{j0}(t + T_j')\rangle$.

There is no need for random phase $e^{i\varphi}$ in this scenario since the second-order coherence $\Gamma_{12} = 0$ for $|(T_1, T_1') - (T_2, T_2')| \gg T_c, T_R$. So, the overall coincidence measurement result is

$$
\begin{aligned}
\langle I(t)I'(t + \tau)\rangle &\propto I_{10}^2(1 + \lambda_1) + I_{20}^2(1 + \lambda_2) + 2I_{10}I_{20} \\
&\quad - I_{10}I_{20}[\gamma_{11}(\Delta T_1 + \tau)\gamma_{22}^*(\Delta T_2 + \tau) + \text{c.c.}] \\
&= I_{10}^2(1 + \lambda_1) + I_{20}^2(1 + \lambda_2) \\
&\quad + 2I_{10}I_{20}\{1 - |\gamma_{11}(\Delta T_1 + \tau)\gamma_{22}(\Delta T_2 + \tau)| \\
&\quad \times \cos[\omega(\Delta T_1 - \Delta T_2) + \Delta\varphi]\},
\end{aligned}
\tag{15}
$$

where $\lambda_j \equiv \langle I_{j0}I_{j0}'\rangle/I_{j0}^2 - 1$ ($j = 1, 2$) describes the intensity fluctuation of each field. This again shows fourth-order interference. A special case is when $T_1' = T_1$, $T_2' = T_2$ and two BSs before the detectors merge into one. This is an unbalanced Mach-Zehnder interferometer (MZI) if the two fields are from the splitting of one field [Fig. 1(c)] or a classical version of the HOM interferometer if the two fields are independent. In this case, we have

$$
\begin{aligned}
\langle I(t)I'(t + \tau)\rangle &\propto I_{10}^2(1 + \lambda_1) + I_{20}^2(1 + \lambda_2) + 2I_{10}I_{20} \\
&\quad - I_{10}I_{20}[\gamma_{11}(\tau)\gamma_{22}^*(\tau) + \text{c.c.}],
\end{aligned}
\tag{16}
$$

where the interference is in the form of a dip as the delay $\Delta T \equiv |T_1 - T_2|$ or detector time delay τ is scanned. Note that, for thermal field of the same kind, we have $\lambda_1 = \lambda_2 = |\gamma_{11}(\tau)|^2 = |\gamma_{22}|^2$ and $I_{10} = I_{20} \equiv I_0$. Then Eq. (16) becomes

$$
\langle I(t)I'(t + \tau)\rangle \propto 4I_0^2,
\tag{17}
$$

showing no interference because the bunching effect of the thermal fields cancels the HOM destructive interference effect. This is only true for stationary thermal fields. In the case of nonstationary pulsed thermal fields, the situation is different because of the requirement of pulse overlap (see later).

(iii) $T_1 \sim T_2'$ and $T_2 \sim T_1'$, but $|(T_1, T_2') - (T_2, T_1')| \gg T_c, T_R$. This scenario is depicted in Fig. 3(b) and we have

$$
\begin{aligned}
\langle V_{10}^*(t &+ T_1)V_{20}(t + T_2)V_{20}(t + T_2' + \tau)V_{10}^*(t + T_1' + \tau)\rangle \\
&\approx \langle V_{10}^*(t + T_1)V_{20}(t + T_2' + \tau)\rangle \\
&\quad \times \langle V_{20}(t + T_2)V_{10}^*(t + T_1' + \tau)\rangle \\
&= \Gamma_{12}(\Delta\bar{T}_1' + \tau)\Gamma_{21}^*(\tau - \Delta\bar{T}_2'),
\end{aligned}
\tag{18}
$$

where $\Delta\bar{T}_1' \equiv T_2' - T_1$, $\Delta\bar{T}_2' \equiv T_2 - T_1'$. Similar to scenario (i), this is for the case of two fields with a common origin. But, in this case, we cannot have random phase $e^{i\varphi}$ because, otherwise, the term above will be zero. On the other hand, since $|(T_1, T_2') - (T_2, T_1')| \gg T_c, T_R$, there is no second-order interference in D1 and D2 in any case so there is no need for the random phase. So, the result of coincidence measurement is

$$
\begin{aligned}
\langle I(t)&I'(t + \tau)\rangle \\
&\propto I_{10}^2 + I_{20}^2 + 2I_{10}I_{20} \\
&\quad - I_{10}I_{20}[\gamma_{12}(\Delta\bar{T}_1' + \tau)\gamma_{21}^*(\tau - \Delta\bar{T}_2') + \text{c.c.}] \\
&= I_{10}^2 + I_{20}^2 \\
&\quad + 2I_{10}I_{20}\{1 - |\gamma_{12}(\Delta\bar{T}_1' + \tau)\gamma_{21}^*(\tau - \Delta\bar{T}_2')| \\
&\quad \times \cos[\omega(\Delta\bar{T}_1' + \Delta\bar{T}_2') + \Delta\varphi]\}.
\end{aligned}
\tag{19}
$$

This scenario is similar to the case of a classical Franson interferometer for thermal fields [13].

Both the results in scenarios (ii) and (iii) depend on τ. So, a time-resolved coincidence measurement is required, which means $T_R \ll T_c$. But interference in these two scenarios will disappear if $T_R \gg T_c$, or the detector's response is too slow to resolve the details of the field fluctuations. This was pointed out in Ref. [11] for the classical Franson interferometer. However, this condition leads to the following scenario.

(iv) $T_R \gg T_c$. Because of the slowness of the detectors, the result of coincidence is an average over detectors' resolving time T_R: $R_c = (1/T_R)\int_{T_R} d\tau \langle I(t)I'(t + \tau)\rangle$. This scenario was discussed in Ref. [4] where it was argued that all higher order correlations are averaged out due to slow detectors. The same argument applies here and the result of coincidence measurement is exactly the same as Eq. (13), that is,

$$
\begin{aligned}
R_c &= \frac{1}{T_R}\int_{T_R} d\tau \langle I(t)I'(t + \tau)\rangle \\
&\propto I_{10}^2 + I_{20}^2 + 2I_{10}I_{20} - I_{10}I_{20}[\gamma_{12}(\Delta T)\gamma_{12}^*(\Delta T') + \text{c.c.}].
\end{aligned}
\tag{20}
$$

Note that although Eq. (13) for scenario (i) and Eq. (20) here have the same form, they have different meaning: Eq. (13) is for $\langle I(t)I'(t+\tau)\rangle$ but is independent of τ, whereas Eq. (20) is after the average over τ. Furthermore, they are derived under different conditions: scenario (i) requires $|(T_1, T_2) - (T_1', T_2')| \gg T_c, T_R$ but makes no assumption about T_R and T_c since the result is independent of τ, whereas scenario (iv) here requires $T_R \gg T_c$ but does not assume anything for T_1, T_2, T_1', T_2' except that nonzero interference terms in Eq. (20) require $|\Delta T|, |\Delta T'| \ll T_c$, which also applies to Eq. (13) for scenario (i). A special case of scenario (iv) is when $T_1 = T_1', T_2 = T_2'$ or $|\Delta T| = |\Delta T'|$. Under this condition, Eq. (20) becomes

$$R_c \propto I_{10}^2 + I_{20}^2 + 2I_{10}I_{20}[1 - |\gamma_{12}(\Delta T)|^2], \qquad (21)$$

where the fourth-order interference is in the form of a dip as the delay ΔT is scanned. This case is exactly the Mach-Zehnder interferometer scheme presented in Ref. [4], which can be used to measure $|\gamma_{12}|$ and the coherence time of an incoming field independent of the photon statistics of the incoming field.

The scenario above can be applied to stellar intensity interferometry [19] when V_{10} and V_{20} are the two fields at two separate locations. Although it can only measure $|\gamma_{12}(\Delta T)|^2$, similar to stellar intensity interferometry, there is no need for time resolution of the detectors and it is suitable for broadband observation.

IV. CASE OF FIELDS IN PULSE TRAINS

For a nonstationary field $V_1(t)$ in the form of a quasi-continuous wave (quasi-cw) train of pulses, the situation somehow becomes relatively simple because the single pulse is usually much faster than the response of the detectors so that the result is a time integral of the single pulse profile. For this case, the field can be written in general as

$$V_1(t) = \sum_j A_j f(t - j\Delta t), \qquad (22)$$

where $f(t)$ is the normalized single pulse profile with a pulse width δt, which we assume is the same for all pulses in the train, A_j is the amplitude of the jth pulse, and $\Delta t (\gg \delta t)$ is the interval between two adjacent pulses. Here, we consider only one polarization and can treat the field as a scalar field. The instantaneous intensity is then

$$\begin{aligned}
I_1(t) = |V_1(t)|^2 &= \sum_{j,k} A_j^* f^*(t - j\Delta t) A_k f(t - k\Delta t) \\
&= \sum_j |A_j f(t - j\Delta t)|^2, \qquad (23)
\end{aligned}$$

where the cross terms are zero because pulse width δt is much smaller than the pulse separation Δt so that there is no overlap between different pulses. The photocurrent from the detector illuminated by this field is then

$$\begin{aligned}
i_1(t) &= \int dt' k(t - t') I_1(t') \\
&= \sum_j |A_j|^2 \int dt' k(t - t') |f(t' - j\Delta t)|^2 \\
&= \sum_j |A_j|^2 k(t - j\Delta t), \qquad (24)
\end{aligned}$$

where $k(t)$ is the detector's response function and we assume that single pulse width of $f(t)$ is much narrower than the detector's response function $k(t)$ so that we can pull $k(t)$ out of the integral. The average photocurrent over a long time of $T (\gg \Delta t)$ is then

$$\begin{aligned}
\langle i_1 \rangle &= \frac{1}{T} \int_T dt\, i_1(t) = QR_p \frac{1}{N} \sum_{j=1}^N |A_j|^2 \\
&= QR_p \langle |A_j|^2 \rangle_j, \qquad (25)
\end{aligned}$$

where $Q \equiv \int dt\, k(t)$ is the total charge produced in the detector for one pulse, R_p is the pulse repetition rate, and $N = [T/\Delta t] = R_p T$ is the number of pulses in time T. $\langle \rangle_j$ is the average over the N pulses. For later calculation, we need to evaluate autocorrelation of the photocurrent within a coincidence window of T_R. The time average is given by

$$\begin{aligned}
R_{11} &= \frac{1}{T} \int_T dt \int_{T_R} d\tau\, i_1(t) i_1(t + \tau) \\
&= \frac{1}{T} \int_T dt \int_{T_R} d\tau \sum_{i,j} |A_i|^2 k(t - i\Delta t) \\
&\quad \times |A_j|^2 k(t + \tau - j\Delta t) \\
&= \frac{1}{T} \int_T dt \int_{T_R} d\tau \sum_j |A_j|^4 k(t - j\Delta t) \\
&\quad \times k(t + \tau - j\Delta t) \\
&= R_p Q^2 \langle |A_j|^4 \rangle_j, \qquad (26)
\end{aligned}$$

where we assume the detectors can resolve different pulses so that $T_R < \Delta t$ and $k(t - i\Delta t)k(t + \tau - j\Delta t) = 0$ if $i \neq j$.

Suppose there is a second field $V_2(t)$ in a pulse train with the same pulse separation Δt:

$$V_2(t) = \sum_j B_j g(t - j\Delta t), \qquad (27)$$

where the amplitude of each pulse is denoted as B_j and the pulse profile is $g(t)$. The coincidence measurement between the two fields is described by the coincidence rate:

$$\begin{aligned}
R_{12} &= \frac{1}{T} \int_T dt \int_{T_R} d\tau\, i_1(t) i_2(t + \tau) \\
&= R_p Q^2 \langle |A_j|^2 |B_j|^2 \rangle_j, \qquad (28)
\end{aligned}$$

whose derivation is similar to Eq. (26).

Now, let us inject the two fields into the unbalanced interferometers shown in Figs. 1 and 3. We consider again the different scenarios of delays as in the stationary case. But we write the delays in terms of pulse separation Δt: $T_1 = N_1\Delta t + d_1/c$, $T_2 = N_2\Delta t + d_2/c$, $T_1' = N_1'\Delta t + d_1'/c$, $T_2' = N_2'\Delta t + d_2'/c$, with $d_1, d_2, d_1', d_2'(< c\Delta t)$ being the extra path delay between two adjacent pulses.

With random phase relation between V_1 and V_2, similar to Eq. (4) in the stationary case, the coincidence measurement between the two outputs of the interferometer is related to eight terms corresponding to two autocorrelation terms $\langle I_1 I_1' \rangle$, $\langle I_2 I_2' \rangle$, two cross-correlation terms $\langle I_1 I_2' \rangle$, $\langle I_2 I_1' \rangle$, and four interference terms. Our discussion of these terms needs to involve detection processes for the case of pulse trains.

For the four intensity correlation terms, their contributions to coincidence measurement can be evaluated in a similar way to Eqs. (26) and (28) and have the form of

$$R_{11'} = R_p Q^2 \langle |A_{j+N_1}|^2 |A_{j+N_1'}|^2 \rangle_j,$$
$$R_{22'} = R_p Q^2 \langle |B_{j+N_2}|^2 |B_{j+N_2'}|^2 \rangle_j,$$
$$R_{12'} = R_p Q^2 \langle |A_{j+N_1}|^2 |B_{j+N_2'}|^2 \rangle_j,$$
$$R_{1'2} = R_p Q^2 \langle |A_{j+N_1'}|^2 |B_{j+N_2}|^2 \rangle_j. \tag{29}$$

The contributions from the four interference terms are more complicated to evaluate. Using Eqs. (22) and (27) for V_1, V_2, we have

$$\int dt' k(t-t') V_1^*(t'+T_1) V_2(t'+T_2)$$
$$= \int dt' k(t-t') \sum_{i,j} A_i^* f^*(t'+T_1-i\Delta t)$$
$$\times B_j g(t'+T_2-j\Delta t)$$
$$= \int dt' k(t-t') \sum_{i,j} A_i^* f^*[t'+d_1/c-(i-N_1)\Delta t]$$
$$\times B_j g[t'+d_2/c-(j-N_2)\Delta t]$$
$$= \beta(\Delta d/c) \sum_j A_{j+N_1}^* B_{j+N_2} k(t-j\Delta t) \tag{30}$$

and

$$\int dt' k(t+\tau-t') V_2^*(t'+T_2') V_1(t'+T_1')$$
$$= \int dt' k(t+\tau-t') \sum_{i,j} B_i^* g^*(t'+T_2'-i\Delta t)$$
$$\times A_j f(t'+T_1'-j\Delta t)$$
$$= \int dt' k(t+\tau-t') \sum_{i,j} A_i f[t'+d_1'/c-(i-N_1')\Delta t]$$
$$\times B_j^* g^*[t'+d_2'/c-(j-N_2')\Delta t]$$
$$= \beta^*(\Delta d'/c) \sum_j B_{j+N_2'}^* A_{j+N_1'} k(t+\tau-j\Delta t) \tag{31}$$

as parts of the contributions in the two detectors from the interference terms. Here, $\beta(\Delta d/c) \equiv \int dt\, f^*(t) g(t+\Delta d/c)$ with $\Delta d \equiv d_2 - d_1$ and $\Delta d' \equiv d_2' - d_1'$.

The time average of the contribution of the first two interference terms to the overall coincidence is then

$$R_{1221} = R_p Q^2 \beta(\Delta d/c) \beta^*(\Delta d'/c)$$
$$\times \langle A_{j+N_1}^* B_{j+N_2} B_{j+N_2'}^* A_{j+N_1'} \rangle_j + \text{c.c.} \tag{32}$$

Similarly, the contribution of the last two interference terms is

$$R_{1212} = R_p Q^2 \beta(\Delta d/c) \beta(\Delta d'/c)$$
$$\times \langle A_{j+N_1}^* B_{j+N_2} A_{j+N_1'}^* B_{j+N_2'} \rangle_j + \text{c.c.} \tag{33}$$

From Eqs. (28), (32), and (33), we sum up all the contributions to obtain the overall coincidence rate for the two outputs of the interferometer:

$$R_c = R_p Q^2 \big\{ \langle |A_{j+N_1}|^2 |A_{j+N_1'}|^2 \rangle_j + \langle |B_{j+N_2}|^2 |B_{j+N_2'}|^2 \rangle_j$$
$$+ \langle |A_{j+N_1}|^2 |B_{j+N_2'}|^2 \rangle_j + \langle |A_{j+N_1'}|^2 |B_{j+N_2}|^2 \rangle_j$$
$$- \big[\beta(\Delta d/c) \beta^*(\Delta d'/c)$$
$$\times \langle A_{j+N_1}^* B_{j+N_2} B_{j+N_2'}^* A_{j+N_1'} \rangle_j + \text{c.c.} \big]$$
$$- \big[\beta(\Delta d/c) \beta(\Delta d'/c)$$
$$\times \langle A_{j+N_1}^* B_{j+N_2} A_{j+N_1'}^* B_{j+N_2'} \rangle_j + \text{c.c.} \big] \big\}. \tag{34}$$

Compared to the stationary case in Eq. (4), we find extra factors of $\beta(\Delta d/c)$, $\beta(\Delta d'/c)$ in the interference terms. Since by Cauchy's inequality we have $|\beta(\tau)|^2 = |\int dt\, f^*(t) g(t+\tau)|^2 \leqslant \int dt |f(t)|^2 \int dt |g(t+\tau)|^2 = 1$, this factor requires the overlap of the pulses from the two input fields at each detector and thus arises from mode match of the temporal profiles of the two fields. It gives rise to the degree of indistinguishability for interference.

Besides the two mode matching factors, the pulsed case is the same as the stationary case and gives rise to the same three scenarios (i–iii). But we do not have the scenario (iv) since we already assume $\Delta t > T_R$.

The dependence of interference terms on the mode match factor can be used in remote sensing to probe the change of the temporal profile when one of the fields passes through a medium, which can cause the change in $f(t)$ or $g(t)$ and thus $\beta(\tau)$, which is related to the visibility of interference. In fact, this was recently demonstrated with an unbalanced Mach-Zehnder interferometer to characterize the influence of dispersion on the temporal modes of the pulses [20]. This corresponds to scenario (ii) with $T_1 = T_1'$, $T_2 = T_2'$ or $\Delta T = \Delta T' \gg T_c, T_R$.

V. SUMMARY AND DISCUSSION

We discussed in this paper various scenarios in fourth-order interference where path differences between interfering fields are much larger than their coherence length. We find phase-sensitive interference fringes may occur in a number of scenarios even though there exist large path differences beyond coherence length. The unbalanced nature of these interference phenomena should find applications in remote optical sensing by interferometric technique.

Although fourth-order correlations are considered, the visibility of interference still depends on second-order correlation functions. Especially, some scenarios require time-resolved two-photon coincidence measurement within the coherence time [scenarios A and B(ii) and B(iii)]. This indicates that these phenomena are in essence originated from second-order coherence either between the two interfering fields or within each field itself. Since the coherence time gives the size of the coherent wave packet in the stationary case, the requirement of time resolution is equivalent to the temporal mode match factor of $\beta(\Delta d)$ in the pulsed case. In some sense,

the size of the coherent wave packet in the stationary case is equivalent to the size of the temporal mode in the pulsed case.

On the other hand, fourth-order correlations do contribute to the results by adding to the baseline in the form of intensity fluctuations in some cases [quantity λ in Eqs. (8) and (15)].

Their effect is to reduce the visibility of interference, as shown in Eq. (11).

[1] J. Haus, *Optical Sensors: Basics and Applications* (Wiley-VCH, Weinheim, 2010).

[2] M. Born and E. Wolf, *Principle of Optics*, 1st ed. (Pergamon Press, New York, 1959); *Principle of Optics*, 6th ed. (Pergamon Press, New York, 1980).

[3] C. K. Hong, Z. Y. Ou, and L. Mandel, Measurement of Subpicosecond Time Intervals Between Two Photons By Interference, Phys. Rev. Lett. **59**, 2044 (1987).

[4] Z. Y. Ou, E. C. Gage, B. E. Magill, and L. Mandel, Fourth-order interference technique for determining the coherence time of a light beam, J. Opt. Soc. Am. B **6**, 100 (1989).

[5] X. Li, L. Yang, L. Cui, Z. Y. Ou, and D. Yu, Observation of quantum interference between a single-photon state and a thermal state generated in optical fibers, Opt. Express **16**, 12505 (2008).

[6] X. Ma, L. Cui, and X. Li, Hong-Ou-Mandel interference between independent sources of heralded ultrafast single photons: Influence of chirp, J. Opt. Soc. Am. B **32**, 946 (2015).

[7] J. D. Franson, Bell Inequality for Position and Time, Phys. Rev. Lett. **62**, 2205 (1989).

[8] Z. Y. Ou, X. Y. Zou, L. J. Wang, and L. Mandel, Observation of Nonlocal Interference in Separated Photon Channels, Phys. Rev. Lett. **65**, 321 (1990).

[9] P. G. Kwiat, W. A. Vareka, C. K. Hong, H. Nathel, and R. Y. Chiao, Correlated two-photon interference in a dual-beam Michelson interferometer, Phys. Rev. A **41**, 2910 (1990).

[10] J. Brendel, E. Mohler, and W. Martienssen, Time-Resolved Dual-Beam Two-Photon Interferences with High Visibility, Phys. Rev. Lett. **66**, 1142 (1991).

[11] Z. Y. Ou and L. Mandel, Classical treatment of the Franson two-photon correlation experiment, J. Opt. Soc. Am. B **7**, 2127 (1990).

[12] V. Tamma and J. Seiler, Multipath correlation interference and controlled-NOT gate simulation with a thermal source, New J. Phys. **18**, 032002 (2016).

[13] Y. S. Ihn, Y. Kim, V. Tamma, and Y.-H. Kim, Second-Order Temporal Interference with Thermal Light: Interference Beyond the Coherence Time, Phys. Rev. Lett. **119**, 263603 (2017).

[14] Y.-R. Fan, C.-Z. Yuan, R.-M. Zhang, S. Shen, P. Wu, H.-Q. Wang, H. Li, G.-W. Deng, H.-Z. Song, L.-X. You, Z. Wang, Y. Wang, G.-C. Guo, and Q. Zhou, Effect of dispersion on indistinguishability between single-photon wave-packets, Photon. Res. **9**, 1134 (2021).

[15] P. Stankus, A. Nomerotski, and A. Slosar, Two-photon amplitude interferometry for precision astrometry, arXiv:2010.09100.

[16] S. M. Tan, D. F. Walls, and M. J. Collett, Nonlocality of a Single Photon, Phys. Rev. Lett. **66**, 252 (1991).

[17] J. D. Monnier, Optical interferometry in astronomy, Rep. Prog. Phys. **66**, 789 (2003).

[18] M. A. Johnson, A. L. Betz, and C. H. Townes, 10-μm Heterodyne Stellar Interferometer, Phys. Rev. Lett. **33**, 1617 (1974).

[19] R. Hanbury-Brown and R. Q. Twiss, A test of a new type of stellar interferometer on Sirius, Nature (London) **178**, 1046 (1956).

[20] W. Zhao, N. Huo, L. Cui, X. Li, and Z. Y. Ou, Propagation of temporal mode multiplexed optical fields in fibers: influence of dispersion, Opt. Express **30**, 447 (2022).